THE ASTROPHYSICAL JOURNAL, 486:681–686, 1997 September 10

INCLINATION EFFECTS IN SPIRAL GALAXY GRAVITATIONAL LENSING

ARIYEH H. MALLER,[1] RICARDO A. FLORES,[2] AND JOEL R. PRIMACK[1]
Received 1997 January 17; accepted 1997 April 15

ABSTRACT

Spheroidal components of spiral galaxies have been considered to be the only dynamically important component in gravitational lensing studies to date. Here we point out that including the disk component can have a significant effect, which depends on the disk inclination, on a variety of lensing properties that are relevant to present studies and future surveys. As an example, we look at the multiple image system B1600+434, which was recently identified as being lensed by a spiral galaxy. We find that by including the disk component, one can understand the fairly large image separation as being caused by the inclination of a typical spiral rather than the presence of a very massive halo. The fairly low magnification ratio can also be readily understood if the disk is included. We also discuss how such lensed systems might allow one to constrain parameters of spiral galaxies such as a disk-to-halo mass ratio and disk mass scale length. Another example we consider is the quasar multiple-lensing cross section, which we find can increase many-fold at high inclination for a typical spiral. Finally, we discuss the changes in the gravitational lensing effects on damped Lyα systems when disk lensing is included.

Subject headings: galaxies: spiral — galaxies: structure — gravitational lensing — quasars: absorption lines

1. INTRODUCTION

Galaxies responsible for gravitational lensing have typically been modeled as one-component systems in which the entire mass distribution of the galaxy lens, visible plus dark matter, is fairly well approximated by a singular isothermal sphere (SIS): $\rho(r) = \rho_0(r_0/r)^2$ (see, e.g., Narayan & Bartelmann 1997). This is probably justified for E/S0 galaxies, where both components have a surface density fairly independent of orientation (a small ellipticity is required only to understand the presence of four-image systems) and the high central density represents the high density of the visible matter. By contrast, in spiral galaxies the disk component has a very different structure from the dark matter halo and the bulge, which results in significantly different projected surface density depending on orientation. Given that the projected surface density of the disk changes by a factor of radius/thickness ~ 15 between a face-on and an edge-on spiral and that the dark and visible components are known to contribute roughly equally to the total mass within 4–5 disk scale lengths, one would expect significant effects on lensing properties for images within a couple of optical radii.

The identification of the lensing galaxy in the double image system B1600+434 as a nearly edge-on spiral by Jaunsen & Hjorth (1997) gives us a perfect example to demonstrate the importance of including the disk component when modeling lensing by spirals. However, an understanding of the lensing geometry of spirals is important for several reasons besides that of modeling observed systems. First, the gravitational lensing effects on damped Lyα systems (DLAS) have been investigated recently (Smette, Claeskens, & Surdej 1997; Bartelmann & Loeb 1996). At least some DLAS are believed to be caused by absorption in protogalactic disks or spiral galaxies (Wolfe 1988, 1997), and if the gas column density falls off exponentially, one is necessarily dealing with lensing within a few exponential scale lengths of the galaxy center, which is where we expect disk lensing to be important. Second, the extra parameters added by introducing a disk component are the physically interesting ones of disk surface density and scale length, so that the observational study of gravitational lensing by spirals will provide new constraints on the distribution of mass in the various components of spirals. Although only a few such systems are currently known, surveys such as the Sloan Digital Sky Survey will catalog a large number of quasars, among which there should be a significant number that are lensed by spiral galaxies. This is why it is also important to understand the effect of disk lensing on statistical properties such as the cross section for multiple-image lensing by spirals.

In this paper, we first explain our method of modeling spiral galaxy lenses as singular isothermal spheres plus infinitesimally thin disks (SIS + disk). We start with the simple example of a disk with constant density to show the effect of adding a disk. We show that such a model fits many of the observations of B1600+434 and discuss the results of modeling, more properly, with an exponential disk. We then discuss the dependence of the lens cross section for multiple lensing of background sources on the inclination of the disk and discuss also how it would enhance the gravitational lensing effects on DLAS. We finish with the conclusions and implications of our work.

2. THE MODEL

We model a spiral galaxy as consisting of two mass components: a spherical halo and an infinitesimally thin disk. We assume that the halo has the density profile of a singular isothermal sphere, while the disk is treated as having surface density that is either constant or falls off exponentially. For simplicity and clarity, we start by treating the case of the constant density disk.

The orientation of the disk defines the coordinate system such that the x- and y-directions are along the major and minor axis, respectively, of the projected disk, and the disk center defines the origin. The model then has six param-

[1] Physics Department, University of California, Santa Cruz, Santa Cruz, CA 95064.
[2] Physics Department, University of Missouri, St. Louis, MO 63121.

eters: the position of the source (β_x, β_y), the inclination of the disk γ_0, the velocity dispersion of the SIS σ_v [the SIS can be equivalently be described by $\rho(r) = \sigma_v^2/2G\pi r^2$], the central surface density Σ_0, and the characteristic length of the disk. For a constant density disk, this characteristic length is the radius of the disk, while in the exponential disk case, this becomes the scale length, R_s. Thus, measuring the position of the lens, the inclination of the disk, the two image positions (θ_x, θ_y), and the magnification ratio completely determines the system.

The inclined circular disk projects onto an ellipse. We denote the axis ratio of an ellipse in general as $\gamma = b/a$, and that of our disk as γ_0. Any point (θ_x, θ_y) external to the ellipse will define a new confocal ellipse with axis ratio γ'. Then the reduced deflection angle, modified from Schramm (1990), is given by

$$\alpha_x = \frac{2\Sigma_0}{\Sigma_{\rm cr}}\,\theta_x\,\frac{1-\gamma'}{1-\gamma_0^2} \tag{1}$$

$$\alpha_y = \frac{2\Sigma_0}{\Sigma_{\rm cr}}\,\theta_y\,\frac{1-\gamma'}{\gamma'(1-\gamma_0^2)}\,. \tag{2}$$

Here $\Sigma_{\rm cr}$ is the usual critical density defined as

$$\Sigma_{\rm cr}^{-1} = \frac{4\pi G D_l D_{ls}}{c^2 D_s} \tag{3}$$

and D_i is the lens, source, or lens-to-source angular diameter distance. If the point (θ_x, θ_y) is inside the disk, then γ' is replaced with γ_0.

3. THE SYSTEM

In the gravitational lens system B1600+434 identified by Jackson et al. (1995), the lensed quasar is at a redshift $z_s = 1.61$, the image separation is 1.″4, and the intensity ratio is $I_{\rm A}/I_{\rm B} = 1.3$ in the radio (in the optical, image B suffers significant extinction). The lens galaxy, identified as a nearly edge-on spiral by Jaunsen & Hjorth (1997), has an estimated photometric redshift $z_l \sim 0.4$ and an axis ratio $a/b = 2.4 \pm 0.2$, or $\gamma_0 = 0.42$. (It is possible that this galaxy is actually an S0 galaxy, as suggested to us by C. Kochanek [1997, private communication], but this will not affect our analysis, as there is still a disk.) To emphasize that this paper is meant as a qualitative exploration of the SIS + disk model, and because z_l is still uncertain, we treat all measurements as if they are exact and include no estimates of errors. The positions of the images in the lens-centered, axes-defined coordinate system are given in Table 1. Note that the lensing galaxy is just 0.″35 from image B. In all of our calculations, we assume $\Omega = 1$, $q_0 = 0.5$, and $H_0 = 100\ h$ km s^{-1} Mpc^{-1}. Furthermore, we calculate angular diameter distances assuming all the matter in the universe is smoothly distributed (see Schneider, Ehlers, & Falco 1992, p. 142).

TABLE 1

IMAGE AND LENS POSITIONS

Object	θ_x (arcsec)	θ_y (arcsec)
Lens.....	0.0	0.0
A	−0.08	1.12
B	0.26	−0.23

Treating the lens as a singular isothermal sphere requires a velocity dispersion of 200 km s^{-1} to account for the image separation. Of course, in this case the lens must be collinear with the images, which is not the case observationally (one would need to introduce some ellipticity in the dark matter distribution to avoid this). However, we can obtain an estimate of the implied relative magnification and the time delay by shifting the lens to the collinear position along a line perpendicular to $\overline{\rm AB}$. The implied time delay is $\Delta t_{\rm AB} = 24\ h^{-1}$ days, and the magnification ratio is 3.8. (The results are similar if the lens position is shifted keeping the ratio of image-lens distances: $\Delta t_{\rm AB} = 22\ h^{-1}$, magnification ratio 3.2.) If one chooses instead to shift the lens to a position that gives the observed relative magnification, the time delay is $\Delta t_{\rm AB} = 5.3\ h^{-1}$ days, but then the images would both be at a similar distance from the lens, which is not as observed.

If instead we model the system as a SIS + constant density disk, we introduce two new parameters: surface density and disk length. The light of the more distant image passes through the disk only $8.7\ h^{-1}$ kpc from its center, so we can start by assuming that the disk length is greater than this and remove one parameter. The equations for a disk with radius greater than $8.7\ h^{-1}$ become

$$\alpha_x = \frac{2\Sigma_0}{\Sigma_{\rm cr}}\,\frac{\theta_x}{1+\gamma_0} \tag{4}$$

$$\alpha_y = \frac{2\Sigma_0}{\Sigma_{\rm cr}}\,\frac{\theta_y}{\gamma_0(1+\gamma_0)}\,, \tag{5}$$

and the lensing potential of the disk in this case is

$$\Psi = \frac{\Sigma_0}{\Sigma_{\rm cr}(1+\gamma_0)}\left(\theta_x^2 + \frac{\theta_y^2}{\gamma_0}\right). \tag{6}$$

Solving for the image positions in Table 1 gives $\Sigma_0 = 7.8 \times 10^8\ h\ M_\odot$ kpc^{-2}, $\sigma_v = 135$ km s^{-1}, and a source position of (0.037, 0.12). The magnification ratio is 1.3, and the time delay is now $\Delta t_{\rm AB} = 43\ h^{-1}$ days (see Fig. 1).

The addition of the disk component has four main effects. First, it breaks the spherical symmetry, which allows the lens not to be collinear with the images. Second, the velocity dispersion in the halo decreases significantly because the disk component contributes to the deflection angle substantially. Third, in this case the magnification ratio is reduced, although in general it depends strongly on the orientation of the images around the lens axis. Finally, the time delay is increased, because the potential now has a term that is quadratic in θ and because the geometric time delays do not cancel out as they do in the SIS case.

It is interesting to note that the surface density of the disk comes out as a reasonable number, although a priori it could have been anything. The deflection caused by a disk with density $\Sigma_0 \sim 10^8$ is of the same scale as that caused by a halo with $\sigma_v \sim 100$ km s^{-1}. Since we observe roughly this amount of luminous matter in the disk, it is clear that the disk's contribution cannot be ignored.

Of course, a disk with constant surface density out to $9\ h^{-1}$ kpc is not a realistic model. We can realistically assume that the disk's surface density falls off as an exponential with scale length R_s. In Figure 2, the images from an exponential disk with $R_s = 5\ h^{-1}$ kpc, $\Sigma_0 = 1.9 \times 10^9\ h\ M_\odot$ kpc^{-2}, and a halo with $\sigma_v = 120$ km s^{-1} are shown. The images are within the position errors for the lens center, and the magnification ratio is roughly correct at 0.97.

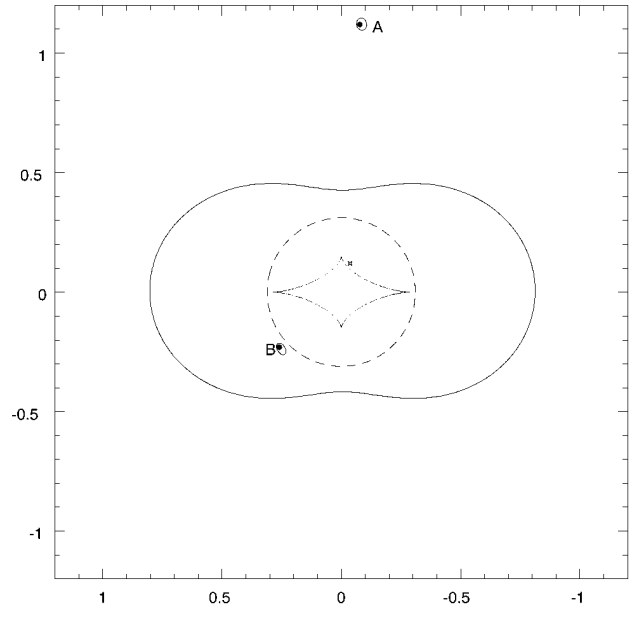

FIG. 1.—Lensing model for B1600+434 by a SIS + *uniform* disk, with disk length greater than 8.7 h^{-1} kpc. The observed images are the black dots. The small contours show the images of a small circular source located at the star symbol in the source plane. Since lensing conserves surface brightness, the relative sizes of the images indicate their magnification ratio. The model magnification ratio calculated from point sources is 1.3. The source position is chosen such that the model images are centered on the observed images. Here $\sigma_v = 135$ km s^{-1} and $\Sigma_0 = 7.8 \times 10^8\ h\ M_\odot$ kpc^{-2}. The dashed curve is the SIS "caustic." The model lens has two caustics: a "tangential" caustic (*dotted line*), and a "radial" caustic that coincides with the SIS caustic. The critical curve corresponding to the "tangential" caustic is shown as the outer solid curve.

Interestingly, we find that the magnification ratio is strongly dependent on the relative orientation of the images and the lens axis. Figure 3 shows the magnification ratio as a function of angle from the *y*-axis. A magnification ratio of

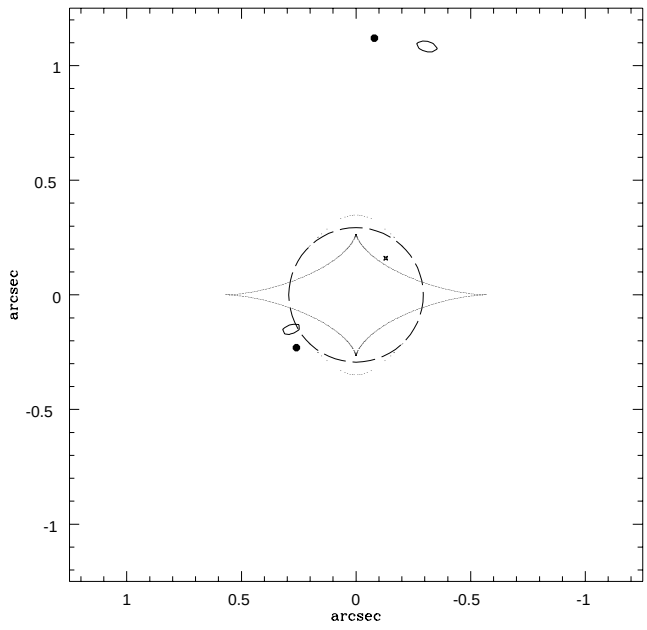

FIG. 2.—Lensing model for B1600+434 by SIS + *exponential* disk. The observed images are the black dots. The images are only slightly off their observed positions and have roughly the correct magnification ratio 0.97. Here, $R_s = 5\ h^{-1}$ kpc, $\Sigma_0 = 1.9 \times 10^9\ h\ M_\odot$ kpc^{-2} and $\sigma_v = 135$ km s^{-1}. Caustics are as in Fig. 1.

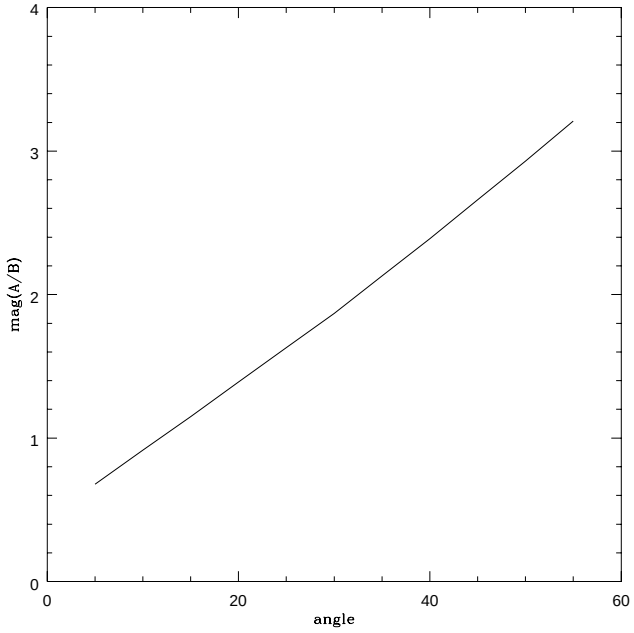

FIG. 3.—Dependence of magnification on source orientation. The magnification ratio is plotted vs. the angle from the y-axis. The source is at a constant distance of 0.″126. The lens parameters are the same as in Fig. 1.

1.3 requires that the source be about 20° off the *y*-axis, which also corresponds to the image orientation found in B1600+434.

In this preliminary study, we have found a surprisingly large disk-to-halo ratio in order to fit the image positions. For the exponential disk, the total disk mass is $3 \times 10^{11}\ h^{-1}\ M_\odot$ compared to a halo velocity dispersion of $\sigma_v = 120$ km s^{-1}. In comparison, standard lore (Binney & Tremaine 1987, p. 17) gives values of $6 \times 10^{10}\ M_\odot$ for the disk mass and 155 km s^{-1} velocity dispersion for the Milky Way, with a disk scale length of 3.5 kpc. While there are large uncertainties in these parameters for the Milky Way, our calculated disk mass does seem excessively large.

Without an understanding of the uncertainties, it is hard to judge how significant these results are. In particular, the inclination we have used (65°; based on the axis ratio measured by Jaunsen & Hjorth 1997) could be much higher, which would tend to decrease the scale length and hence the total disk mass. A preliminary inspection of *Hubble Space Telescope* (*HST*) archival images of B1600+434 reveals a dust lane nearly bifurcating the disk, suggesting an inclination greater than 80°. However, if the large disk mass did turn out to be significant, it may be evidence that the dark matter halo is flattened (see, for example, Olling 1996; Sackett 1996; Rix 1996) and the nonspherically situated dark matter is contributing to what we have assumed is a visible matter disk. It is also possible that the dark matter halo may have a core radius, and since the lensing is mostly sensitive to the matter inside the images, the σ_v we are measuring is lower than the value one would use to characterize this galaxy. We are preparing to address these issues in a more detailed study to follow.

4. OTHER EFFECTS OF INCLUDING A DISK COMPONENT

The inclination of the disk can have a dramatic effect on the lens cross section for multiple lensing of background

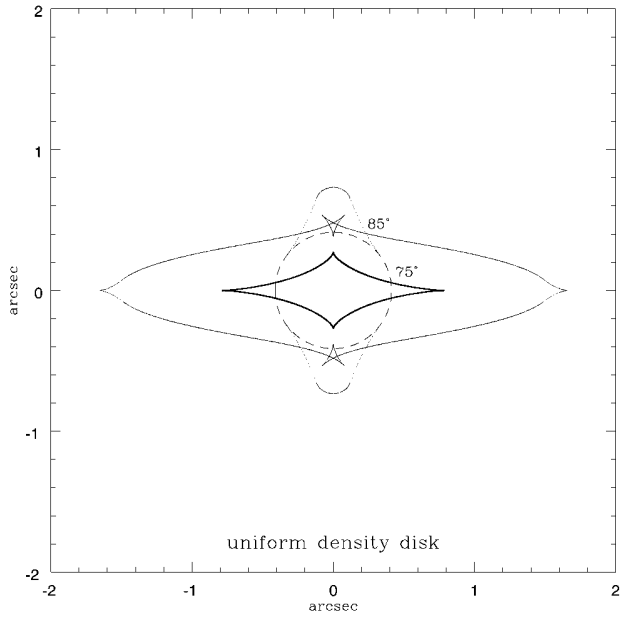

FIG. 4.—Dependence of multiple-lensing cross section on disk inclination. Here the lens has a halo with $\sigma_v = 155\ h$ km s^{-1} and a uniform density disk with mass $M_{\rm disk} = 10^{11}\ h^{-1}\ M_\odot$ and radius $R_{\rm disk} = 8\ h^{-1}$ kpc. The dashed circle represents the caustic of the SIS halo. When inclined at 75°, the "tangential" caustic is the thick line and the "radial" caustic coincides with the dashed circle. When inclined at 85°, the "tangential" caustic is the thin line and the "radial" caustic is the dotted line that joins the dashed circle. (A source behind the tip of the arrowlike region would have six images.) Here, $\Omega = 1$, $z_s = 1.6$, $z_l = 0.4$, $V_c^{\rm SIS} = 220$ km s^{-1}, $M_{\rm disk} = 10^{11}\ M_\odot$, $R_{\rm disk} = 8$ kpc.

sources, as we show in Figure 4. Here we again model the disk with constant surface density, but we choose parameters more representative of an L_*-type spiral.

In this case it is possible to obtain a simple expression for the critical inclination, $\gamma_c = \cos\theta_c$, at which the cross section begins to exceed that of the SIS halo alone. Note that this occurs when the inner caustic emanating from the disk touches the SIS caustic. If the inclination slightly exceeds θ_c, then we can have a source just outside the SIS caustic and just inside the disk caustic (see the 75° curve in Fig. 4). A source at this location, $(\beta_x, \beta_y) = (\alpha_{\rm SIS}, 0)$ with $\alpha_{\rm SIS} = (D_{ls}/D_s)4\pi(\sigma_v/c)^2$, has three images. Using the lens equation

$$\beta = \theta - \alpha_{\rm disk} - \alpha_{\rm SIS} \tag{7}$$

we see that, assuming the disk radius is larger than $\alpha_{\rm SIS}$, one image is at

$$\theta_{x0} = \frac{2\alpha_{\rm SIS}}{1 - [2\Sigma_0/\Sigma_{\rm cr}(1+\gamma_c)]} \quad \text{and} \quad \theta_y = 0\ . \tag{8}$$

Because we know that the images will merge as the source passes through the caustic, we know that the other two images must be close to the first one. Thus, there are two images at $\theta_x \approx \theta_{x0}$ and $\pm\theta_{y0}$, where $\theta_{x0} \gg \theta_{y0}$. For these two images, the lens equation requires

$$\frac{\alpha_{\rm SIS}}{\theta_{x0}} + \frac{2\Sigma_0}{\Sigma_{\rm cr}\gamma_c(1+\gamma_c)} = 1 \tag{9}$$

independently of θ_{y0}. Therefore,

$$\gamma_c = \cos\theta_c = \frac{1}{2}\left[\sqrt{1 + 20\,\frac{\Sigma_0}{\Sigma_{\rm cr}} + \left(\frac{2\Sigma_0}{\Sigma_{\rm cr}}\right)^2} - 1 - 2\,\frac{\Sigma_0}{\Sigma_{\rm cr}}\right] \tag{10}$$

gives the critical inclination.

In Figure 4, we show two inclinations for a disk of mass $M_{\rm disk} = 10^{11}\ h^{-1}\ M_\odot$ and radius $R_{\rm disk} = 8\ h^{-1}$ kpc inside a SIS halo with $\sigma_v = 155$ km s^{-1}. For this choice of parameters, $\theta_c \approx 73°$. Thus, at an inclination of 75°, the cross section shows a modest increase. By contrast, at 85° we find a very large increase—a factor of ≈ 3.5 over that of the SIS halo alone. The disk model is not realistic, of course, but the effect is quantitatively similar for an exponential disk. In particular, θ_c is still fairly well approximated by equation (10).

Whether this increase in cross section significantly increases the fraction of spiral galaxies responsible for multiple image lensing depends on the amount of mass in the disk. In Figure 5, one sees that for parameters such as those quoted for the Milky Way, the average (integrated over $\cos\theta_i$) increase is small, roughly 25%, while for a heavy disk such as our model of B1600+434, the average cross section increases by $\sim$90%. However, since the amplification also increases with disk inclination, the brightest quasars lensed by disk galaxies will probably have highly inclined disks, especially if the disks are massive. Thus, the fraction of lenses that are spirals and their relative inclinations will place strong constraints on the total disk mass. We shall discuss these issues in more detail in a subsequent publication.

The last problem we study here is how our results would affect the gravitational lensing effects on DLAS. Bartelmann & Loeb (1996) and Smette (1995) have pointed out that gravitational lensing could significantly affect the

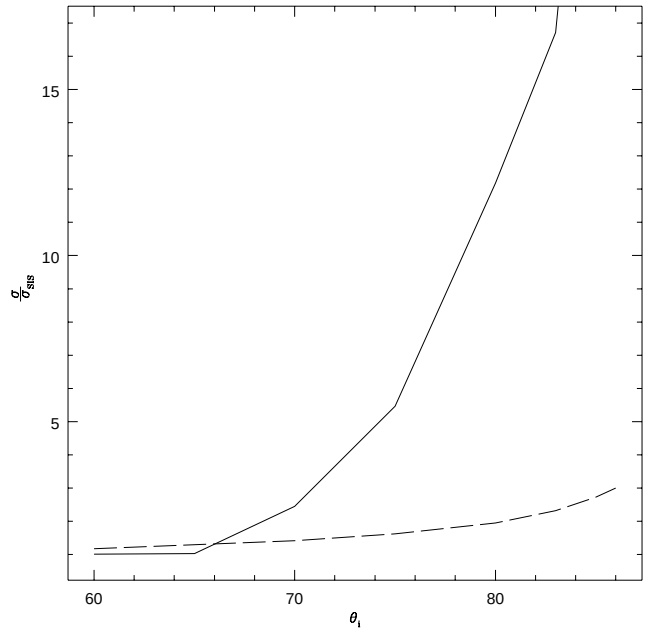

FIG. 5.—Increase in multiple image cross section to SIS alone as a function of inclination for a SIS + exponential disk model. The solid line is for a massive disk such as that found for B1600+434 (see Fig. 2). The broken line is for a less massive disk such as a Milky Way–type galaxy with $M_{\rm disk} = 6 \times 10^{10}\ h^{-1}\ M_\odot$ and radius $R_{\rm disk} = 3.5\ h^{-1}$ kpc.

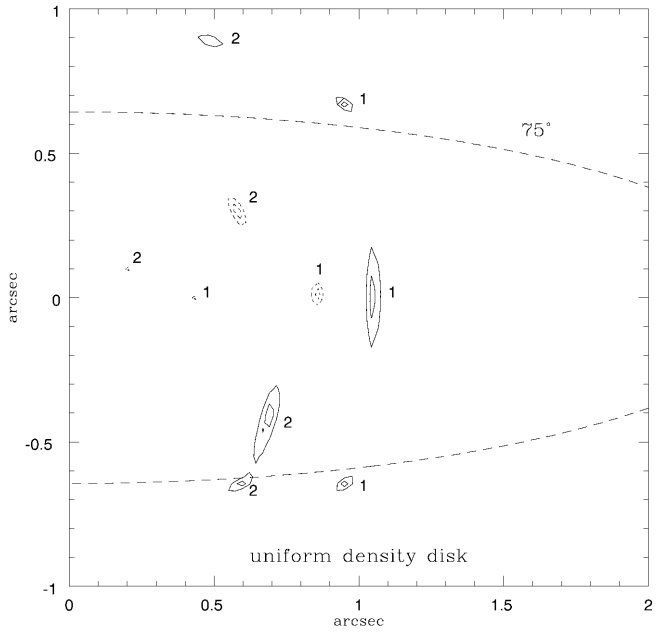

FIG. 6.—Dependence of magnification and bending angle on disk inclination. The solid lines are image contours of two circular sources (1 and 2) at positions marked by the star symbols. Here the disk is as in Fig. 4, inclined at 75°. The dashed contours mark where the image contours lie for the SIS halo alone. The dotted line marks the edge of the constant density disk. Here, $\Omega = 1$, $z_s = 1.6$, $z_l = 0.4$, $V_c^{\rm SIS} = 220$ km s^{-1}, $M_{\rm disk} = 10^{11}\,M_\odot$, $R_{\rm disk} = 8$ kpc.

observed properties of DLAS for two reasons. First, magnification bias significantly enhances the probability of observing damped absorption in a QSO spectrum. Second, there is a cutoff in the observed column density owing to light bending, which makes it far more likely to observe absorption that occurs at large radii. Since the column density of absorbing H I falls off exponentially, this significantly effects the observed column densities.

In their studies, Smette et al. (1997) and Bartelmann & Loeb (1996) treated the spiral disk as essentially massless for lensing purposes. We find that including the disk lensing will significantly enhance both of these effects, as we show in Figure 6. There we show the effects of adding disk lensing on the magnification and impact parameters of two sources. First, note that there is a significant increase in the magnification of the image that precisely occurs on the surface of the disk. For the example shown, the L_*-type disk considered above, the point-source magnification increase is $\approx 5.2(3.0)$ for the source at position 1 (2). Second, there is an increase in the impact parameter, which would result in further reduction of the observed column density. These results are typical of what we find at high inclinations of 60°–80°. Note that the increased magnification by inclined disks increases the likelihood of lensing in this configuration; this could obviate the need for rather thick disks (see, e.g., Wolfe 1997) to account for the metal line systems seen in DLAS. Also, one must be aware that unresolved multiple images may pass through the same disk at various places, which complicates the reconstruction of the absorbing system.

A complete analysis is now far more involved, as one must model the disk as an exponential disk, average over the observed magnification, and average over the disk inclination. The effects of dust in obscuring images (as clearly demonstrated in the relative reddening of image B to A in B1600+434) must also be included. We will discuss the full problem in a subsequent publication.

5. CONCLUSIONS

We have shown that the inclusion of a disk component in a spiral gravitational lens model has significant effects that cannot be ignored. Our results imply that a host of issues, ranging from the ability of spirals to lens QSOs to detailed properties of lens systems, should be reconsidered to properly include the lensing effects of their disks. We have shown, as an example, that a SIS + disk model can account for the observations of the B1600+434 system with fairly reasonable parameters. The implications of our results are that a velocity dispersion σ_v significantly smaller than the SIS prediction of 200 km s^{-1} and a time delay greater than 1 month are to be expected.

With more data and more detailed analysis, the modeling of multiply imaged systems that are lensed by spiral galaxies will constrain the relative amounts of matter in the disk and halo when disk lensing is included. However, because of the dependence on new parameters, further study will be necessary before such systems can give an unambiguous measurement of the Hubble parameter h. We have also noted that the disk contribution to lensing will make the amplification and bypass effects on the observed distribution of DLAS in bright QSOs even more pronounced at high column densities.

After the first version of this paper was posted on the preprint archive, a preprint was posted by Wang & Turner (1997), who discuss critical curves and caustics of inclined, constant density disks. Their equations and figures can be seen to be the same as ours if one carefully scales appropriately by the Hubble constant h and notices that they have calculated angular diameter distances with all the matter in the universe in clumps, while we have assumed it to be distributed smoothly.

This work has been supported by NSF grant PHY 96-00239 at the University of Missouri, St. Louis, by NSF grant PHY 94-02455, and by a NASA ATP grant at the University of California, Santa Cruz. A. M. also acknowledges GAANN support. The authors are grateful for helpful suggestions from the referee, Matthias Bartelmann; for help from Raja Guhathakurta and Steve Vogt in interpreting the *HST* archival image of B1600+434; and correspondence from A. O. Jaunsen, Chris Kochanek, and Tom Schramm.

REFERENCES

Bartelmann, M., & Loeb, A. 1996, ApJ, 457, 529
Binney, J., & Tremaine, S. 1987, Galactic Dynamics (Princeton: Princeton Univ. Press)
Jackson, N., et al. 1995, MNRAS, 274, L25
Jaunsen, A. O., & Hjorth, J. 1997, A&A, 317, L39
Narayan, R., & Bartelmann, M. 1997, in Formation and Structure of the Universe, ed. A. Dekel & J. P. Ostriker (Cambridge: Cambridge Univ. Press), in press
Olling, R. P. 1997, in Aspects of Dark Matter and Astro- and Particle Physics, ed. H. V. Klapdor-Kleingrothaus & Y. Ramachers (Singapore: World Scientific), in press
Rix, H.-W. 1996, in Unsolved Problems of the Milky Way, ed. L. Blitz & P. Teuben (Dordrecht: Kluwer), 23
Sackett, P. D. 1996, in Astrophysical Applications of Gravitational Lensing, eds. C. S. Kochanek & J. N. Hewitt (Dordrecht: Kluwer), 165

Schneider, P., Ehlers, J., & Falco, E. E. 1992, Gravitational Lenses (New York: Springer)
Schramm, T. 1990, A&A, 231, 19
Smette, A. 1995, in QSO Absorption Lines, ed. G. Meylan (New York: Springer), 275
Smette, A., Claeskens, J. F., & Surdej, J. 1997, New Astron., in press
Wang, Y., & Turner, E. L. 1997, preprint (astro-ph/9702078)
Wolfe, A. M. 1988, in QSO Absorption Lines: Probing the Universe, ed. J. C. Blades, D. A. Turnshek, & C. A. Norman (Cambridge: Cambridge Univ. Press), 297
———. 1997, in Critical Dialogues in Cosmology, ed. N. Turok (Singapore: World Scientific), in press